JOURNAL OF CATALYSIS 69, 18–31 (1981)

Solid-Electrolyte-Aided Study of the Ethylene Oxidation on Polycrystalline Silver

MICHAEL STOUKIDES AND COSTAS G. VAYENAS

Massachusetts Institute of Technology, Cambridge, Massachusetts 02139

Received July 23, 1980; revised December 2, 1980

The oxidation of ethylene on porous polycrystalline Ag films supported on stabilized zirconia was studied in a CSTR at temperatures between 250 and 450°C and atmospheric pressure. The technique of solid-electrolyte potentiometry (SEP) was used to monitor the chemical potential of oxygen adsorbed on the catalyst. The rates r_1, r_2 of ethylene epoxidation and combustion were found to satisfy $r_1 = K_1K_{ET}P_{ET}/(1 + K_{ET}P_{ET})$, $r_2 = K_2K_{ET}P_{ET}/(1 + K_{ET}P_{ET})$, respectively, with $K_{ET} = 8.7 \cdot 10^{-4} \exp(5800/T)$ bar^{-1}, $K_1 = 0.28 \exp(-7300/T)$ mole/s, and $K_2 = 2. \cdot 10^2 \exp(-11100/T)$ mole/s on a porous film that could adsorb a total of $2 \cdot 10^{-6}$ moles O_2. The steady-state atomic oxygen activity a_O satisfies the equation $P_{O_2}^{1/2}/a_O = 1 + KP_{ET}/P_{O_2}$ with $K = 3.4 \cdot 10^{-5} \exp(7800/T)$. The effect of carbon dioxide on the catalytic oxidation of ethylene was also studied at temperatures between 250 and 400°C and atmospheric total pressure. Over the range of conditions investigated CO_2 was found to inhibit ethylene epoxidation only, without measurably affecting the rate of complete oxidation to CO_2 or the potentiometrically measured atomic oxygen activity on the Ag catalyst. The inhibiting effect of CO_2 on the rate of ethylene epoxidation r_1 can be described by $r_1/r_1^\circ = P_{O_2}/(P_{O_2} + K'P_{CO_2})$, where r_1° is the rate of epoxidation for vanishingly low P_{CO_2} and $K' = 1.2 \cdot 10^{-5} \cdot \exp(6600/T)$. A simple mechanism is proposed which explains all the experimental observations.

INTRODUCTION

Due to the industrial importance of the ethylene epoxidation on silver, the kinetics and mechanism of this reaction have been studied extensively. Work prior to 1974 has been reviewed by Kilty and Sachtler (*1*). Despite the large number of investigations and some very interesting recent experimental findings (*2–9*) no generally accepted reaction mechanism has yet been established.

Ethylene and oxygen react on silver catalysts to produce ethylene oxide and CO_2. It is well established that even with short contact times CO_2 comes both from direct oxidation of ethylene as well as from the secondary oxidation of ethylene oxide (*10, 11*). The reaction network can thus be written as

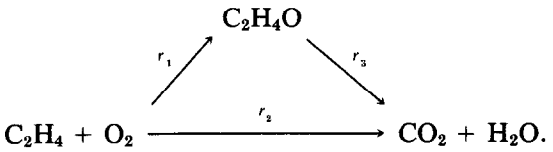

The kinetics and mechanism of the secondary oxidation of ethylene oxide to CO_2 and H_2O on polycrystalline Ag films supported on stabilized zirconia (*12*) have been studied separately. The subject of this paper is the kinetics of the two ethylene oxidation reactions r_1 and r_2. The experimental approach was to combine kinetic studies in a CSTR with simultaneous *in situ* solid-electrolyte potentiometric (SEP) mea-

0021-9517/81/050018-14$02.00/0

surement of the thermodynamic activity of oxygen on the working silver catalyst.

Twigg reported the first thorough kinetic study of ethylene oxidation on silver (*10, 11*). He suggested an Eley–Rideal-type mechanism between gaseous ethylene and atomically adsorbed oxygen. It has been well established, however, that several forms of chemisorbed oxygen exist on silver (*1, 2, 19*) and that ethylene adsorbs on oxygen-covered silver (*6–8*).

Force and Bell have studied the infrared spectra of species adsorbed on silver during ethylene oxidation (*6*) and examined the relationship of these species to the reaction mechanism (*7*). Kummer has studied the reaction kinetics on different Ag crystallographic planes and found little difference in activity and selectivity (*14*). Carberry *et al.* (*3*) have found that the selectivity to ethylene oxide increases by γ-preirradiation of the catalyst. Harriot *et al.* (*8, 15*) have studied extensively support and crystal size effects on activity and selectivity. Cant and Hall (*4*) used ^{14}C to study oxygen exchange between ethylene and ethylene oxide and found that ethylene oxide oxidation to CO_2 is much slower than direct CO_2 formation from ethylene oxidation, in agreement with previous kinetic studies (*10, 11, 13*). In a recent communication, Dettwiller *et al.* (*16*) provide detailed kinetic expressions for the three initial rates r_1, r_2, and r_3 for silver supported on pumice (*16*).

The inhibiting effect of reaction products and other species on the rate of ethylene oxidation on silver has been the subject of considerable study. Hydrocarbons (*33*) have been reported to retard both ethylene epoxidation and combustion.

Kurilenko *et al.* (*18*) and Metcalf and Harriot (*35*) have suggested that CO_2 inhibits both ethylene epoxidation and deep oxidation. However, Hayes has found that CO_2 has an inhibiting effect on ethylene epoxidation only (*17*). Nault *et al.* (*34*) suggested that CO_2 inhibits both reactions but the effect is much larger on the ethylene epoxidation reaction.

In the present work previous observations and kinetic measurements are examined in light of the directly measured activity a_O of oxygen on the silver catalyst. Originally proposed by C. Wagner the technique of solid-electrolyte potentiometry (SEP) allows for an *in situ* measurement of a_O on metal catalysts (*20*). It utilizes a solid-electrolyte oxygen concentration cell with one electrode also serving as the catalyst for the reaction under study. The technique has been used in conjunction with kinetic measurements to study SO_2 oxidation on noble metals (*21*), ethylene oxidation on platinum (*22*), and ethylene oxide oxidation on Ag (*12*). An indirect measurement of the activity of oxygen a_O adsorbed on Ag has been obtained by Imre (*23*). Solid-electrolyte cells similar to the one described here have been used (a) by Mason *et al.* to enhance the rate of the NO catalytic decomposition on Pt by oxygen "pumping" (*24*), (b) by Farr and Vayenas to electrocatalytically oxidize ammonia and cogenerate electrical energy and nitric oxide (*25, 26*), (c) by Stoukides and Vayenas to enhance the rate and selectivity of ethylene oxidation on silver by oxygen "pumping" (*27*). In the present work attention is focused on the open circuit emf of the cell which permits direct calculation of a_O on the metal catalyst.

EXPERIMENTAL

The experimental apparatus shown in Fig. 1 is the one used to study the oxidation of ethylene oxide and has been described in detail elsewhere (*12, 22*). The porous silver catalyst film was deposited on the flat bottom of an 8% yttria-stabilized zirconia tube. It had a superficial area of 2 cm^2 and a total surface area of approximately 1900 cm^2. The silver catalyst film preparation and characterization procedure has been described previously (*12*). A similar Ag film was deposited on the outside bottom wall of the zirconia tube. This Ag film was exposed to air and served as the reference electrode.

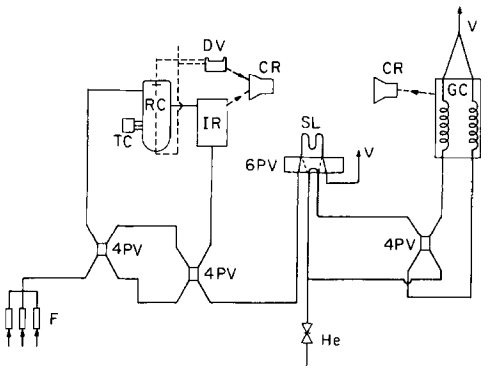

FIG. 1. Schematic diagram of the apparatus. (F) Calibrated feed flowmeters, (4PV) four-port valve, (6PV) six-port valve, (RC) reactor cell, (TC) temperature controller, (IR) infrared CO analyzer, (DV) differential voltmeter, (SL) sampling loop, (GC) gas chromatograph, (CR) strip-chart recorder, (V) vent.

The continuous-flow reactor used has been previously described and shown to be well mixed (CSTR) over the range of flow rates employed in the present study (*22*). The residence time distribution curve of the reactor obtained with an ir CO_2 analyzer is shown in Fig. 2.

The open-circuit emf of the oxygen concentration cell was measured with a J. Fluke voltmeter with an input resistance of 10^8 ohms and infinite resistance at nul. The bottom of the stabilized zirconia tube was diamond polished to a thickness of ~200 μm so that the resistance of the oxygen concentration cell was below 10^3 ohms even at the lowest temperatures used. The correct performance of the cell as an oxygen concentration cell was verified by introducing into the reactor various air–N_2 mixtures of known P_{O_2} and obtaining agreement within 1–2 mV with the Nernst equation.

$$E = (RT/2F)\ln[P_{O_2}/(0.21)]^{1/2}. \quad (1)$$

Reactants were Matheson certified standards of ethylene in nitrogen, CO_2 in nitrogen, and Matheson zero-grade air. They could be further diluted in N_2 by means of a gas mixer to maintain the partial pressure of either ethylene or oxygen constant at desired values. The mixer flowmeters were calibrated in order to measure accurately the total flow rate. Ethylene oxide and CO_2 diluted in N_2 could also be added to the feed, when desired, by means of a fourth calibrated flowmeter.

Reactants and products were analyzed by means of a Perkin–Elmer gas chromatograph with a TC detector. A Porapak Q column was used to separate air, CO_2, ethylene, and ethylene oxide. A molecular sieve 5A column was used to separate N_2 and O_2. The carbon and oxygen balance between reactants and products was con-

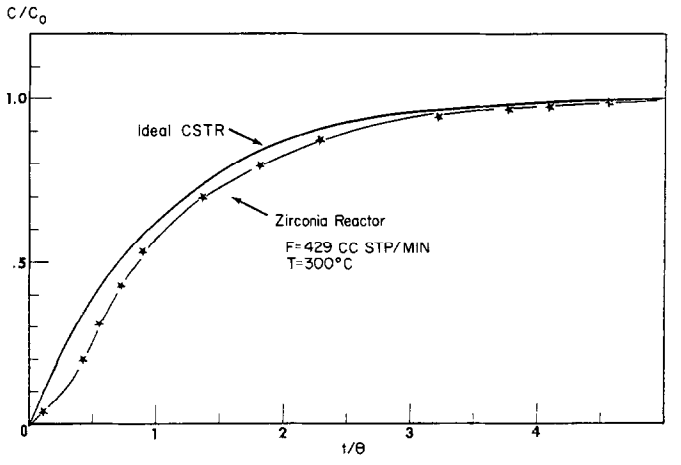

FIG. 2. Reactor response to a step change in inlet CO_2 concentration. Mean residence time Θ = 2.18 s. Detector: ir CO_2 analyzer.

sistent within 1%. The concentration of CO_2 in the products was also monitored by a Beckman 864 ir analyzer.

Measurement of the Oxygen Activity

The technique of solid-electrolyte potentiometry (SEP), previously employed to study SO_2 oxidation on noble metals (*21*) and ethylene oxidation on Pt (*22*), was used to measure *in situ* the thermodynamic activity of oxygen on the Ag catalyst. The open circuit emf of the solid-electrolyte cell utilized here is

$$E = [1/4F]\,[\mu_{O_2(Ag)\ \text{catalyst}} - \mu_{O_2(Ag)\ \text{reference}}], \quad (2)$$

where F is the Faraday constant and $\mu_{O_2(Ag)}$ is the chemical potential of oxygen adsorbed on the Ag electrodes. This is derived on the assumption that the stabilized zirconia solid electrolyte is a purely anionic (O^{2-}) conductor and that the dominant exchange current reaction involves O^{2-} and adsorbed oxygen. Equation (2) includes as a limiting case the usual Nernst equation

$$E = \frac{RT}{4F} \ln \frac{P'_{O_2}}{P_{O_2}} \quad (3)$$

which is valid only when no chemical reaction involving the gas phase proceeds at the electrode surface (*28*). In the general case it is the activity of oxygen adsorbed on the electrodes rather than the gas-phase oxygen activity which determines the open-circuit emf (*29*).

The chemical potential of oxygen at the reference electrode which is in contact with air (P_{O_2} = 0.21 bar) is given by

$$\mu_{O_2(Ag)\ \text{reference}} = \mu^{\circ}_{O_2(g)} + RT \ln(0.21), \quad (4)$$

where $\mu^{\circ}_{O_2(g)}$ is the standard chemical potential of oxygen at the temperature of interest. One can define the activity of oxygen atoms on the catalyst a_O by a similar equation

$$\mu_{O_2(\text{catalyst})} = \mu^{\circ}_{O_2(g)} + RT \ln a_O{}^2. \quad (5)$$

Therefore $a_O{}^2$ expresses the partial pressure of gaseous oxygen that would be in thermodynamic equilibrium with oxygen atoms adsorbed on the silver surface, if such an equilibrium were established.

Combining Eqs. (1), (3), and (4), a_O ($bar^{1/2}$) is given by

$$a_O = 0.21^{1/2} \exp(2FE/RT). \quad (6)$$

If equilibrium is established between gaseous oxygen in the reactor and oxygen on the catalyst, then

$$a_O{}^2 = P_{O_2}.$$

RESULTS

Kinetic Measurements

The kinetics were studied extensively at temperatures between 250 and 450°C, ethylene partial pressures between 10^{-3} and $2. \cdot 10^{-2}$ bar, and oxygen partial pressures between $1.5 \cdot 10^{-2}$ and $15. \cdot 10^{-2}$ bar.

After an initial induction period which lasted approximately 48 h the catalyst activity and selectivity remained constant within 2% for at least 10 weeks.

The absence of external diffusional effects was verified by varying the total flow rate between 150 and 400 cm^3 STP/min at quasi-constant gas composition and observing no measurable change on the global rates or on the electrochemically measured surface oxygen activity a_O. Internal diffusional effects were also absent. This was verified by using three different reactors with porous Ag film thicknesses varying roughly between 3 and 20 μm and observing no difference (<1–2%) in the surface oxygen activity at the same temperature and gas-phase composition. Since the surface oxygen activity a_O is measured at the bottom of the porous Ag film, i.e., at the gas–metal–zirconia interline, this proves the absence of internal diffusional effects.

The three independent reaction rates r_1, r_2 (moles C_2H_4/s), and r_3 (moles C_2H_4O/s) defined in the Introduction are calculated as follows from the raw kinetic data of the CSTR: First, we calculated r_3 using the partial pressure of ethylene oxide P_{ETOX} in

the products and the rate expression obtained in our previous work for the same catalyst (*12*)

$$r_3 = K_3 \cdot K_{ETOX}^{\rightarrow} \cdot P_{ETOX}^2/(1 + K_{ETOX}P_{ETOX}^2)$$

with

$$K_3 = 14.4 \exp(-10200/T) \text{ mole/s}$$

and

$$K_{ETOX} = 3.3 \cdot 10^{-5} \exp(10600/T) \text{ bar}^{-2}.$$

As it turns out because of the low conversions employed in the present study (<30%), i.e., due to the relatively high P_{ET} and low P_{ETOX}, r_3 is of the order of 1% of r_1 and r_2. This was again verified by introducing ethylene oxide and oxygen in the reactor at the same P_{ETOX} and space velocities employed in the main kinetic study. The rate r_3 is therefore much smaller than r_1 and r_2 and in most cases small enough to be neglected (<1%). This is also demonstrated by the fact that over the range of space times employed in the present study (3–15 s), selectivity (moles ETOX produced/moles ethylene reacted) was practically space time independent. However it might be anticipated that the presence of ethylene alters the value of r_3 from that obtained in the separate ethylene oxide oxidation study (*12*). This effect has been studied separately and found to be small and in the direction of decreasing r_3. Therefore r_3 can be neglected for the purposes of the present investigation, i.e., practically all CO_2 produced comes from direct ethylene oxidation. This has been suggested by previous workers too (*4, 10, 11, 13*).

Thus taking into account that the reactor is a CSTR the reaction rates r_1, r_2 can be calculated from the appropriate mass balances:

$$r_1 - r_3 \approx r_1 = G \cdot X_{ETOX}, \quad (7)$$

$$r_2 + r_3 \approx r_2 = \tfrac{1}{2} \cdot G \cdot X_{CO_2}, \quad (8)$$

where X_{ETOX}, X_{CO_2} are the exit mole fractions of ethylene oxide and CO_2 and G is the total molar flow rate.

The values of r_1 and r_2 thus obtained were also found to satisfy within 1% the mass balance requirement

$$r_1 + r_2 = G[X_{ET,IN} - X_{ET,OUT}]. \quad (9)$$

Due to the high partial pressure of diluent N_2 (~0.7 bar) and the low conversion, volume changes due to reaction were calculated to be negligible (<0.3%). Each kinetic point presented here is the average of two measurements usually differing less than 1–2%.

The rate of ethylene oxide production r_1 is plotted in Fig. 3 vs the partial pressure of

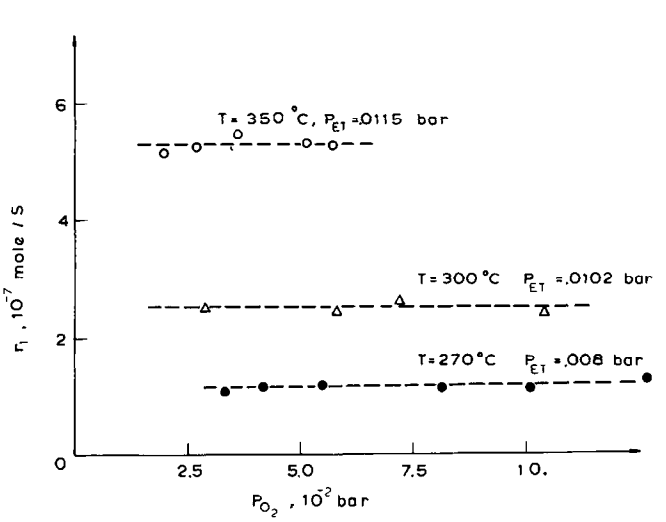

FIG. 3. Rate of ethylene epoxidation r_1 vs P_{O_2} at constant P_{ET} and temperature.

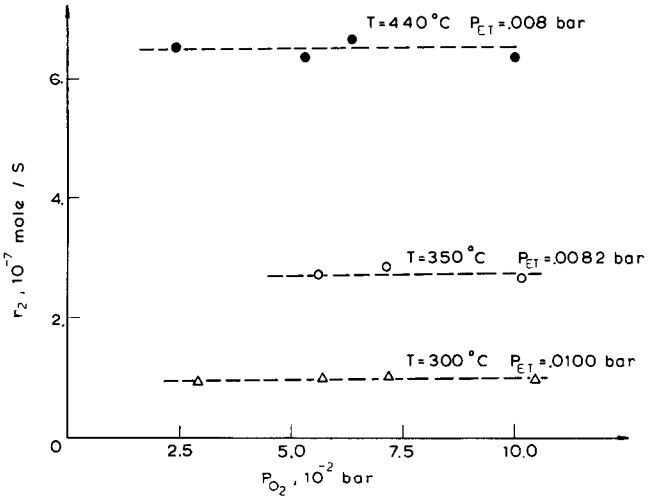

FIG. 4. Rate of ethylene oxidation to CO_2 r_2 vs P_{O_2} at constant P_{ET} and temperature.

oxygen at constant T and P_{ET}. The rate of deep ethylene oxidation r_2 is plotted vs P_{O_2} in Fig. 4. Clearly both r_1 and r_2 are zero order in oxygen over the range of P_{O_2} values investigated.

Figure 5 exhibits the dependence of r_1, r_2 on P_{ET} at 440°C which is the highest temperature studied. Both rates are first order in ethylene.

However at lower temperatures this simple first-order dependence on ethylene disappears as shown in Figs. 6 and 7.

It was found that all the kinetic data could be expressed rather accurately by the rate expressions

$$r_1 = K_1 K_{ET} P_{ET}/(1 + K_{ET} P_{ET}), \quad (10)$$

$$r_2 = K_2 K_{ET} P_{ET}/(1 + K_{ET} P_{ET}) \quad (11)$$

with

$$K_1 = 0.28 \exp(-7300/T) \text{ mole/s}, \quad (12)$$

$$K_2 = 2. \cdot 10^2 \exp(-11100/T) \text{ mole/s}, \quad (13)$$

$$K_{ET} = 8.7 \cdot 10^{-4} \exp(5800/T) \text{ bar}^{-1}. \quad (14)$$

It should be noted that according to these rate expressions which account for the retarding effect of ethylene, the selectivity depends very little on gas composition at constant temperature, at least over the range of gas-phase compositions investigated. This is shown in Fig. 8.

Oxygen Activity during Reaction

With inert-O_2 mixtures present in the

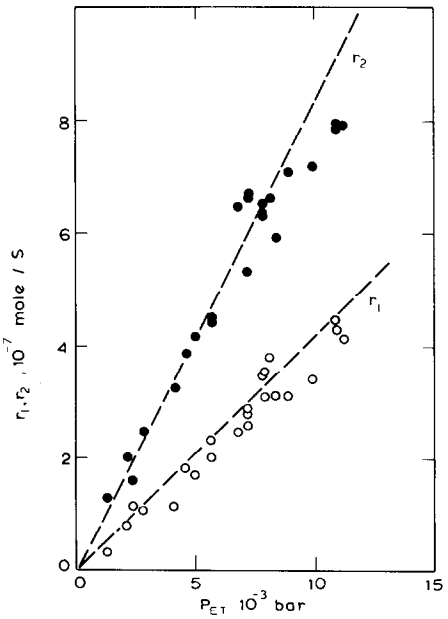

FIG. 5. Rates of ethylene epoxidation (r_1) and combustion (r_2) vs P_{ET} at 440°C. The partial pressure of oxygen varies between $1.5 \cdot 10^{-2}$ and $15 \cdot 10^{-2}$ bar. Broken lines correspond to Eqs. (10)–(14).

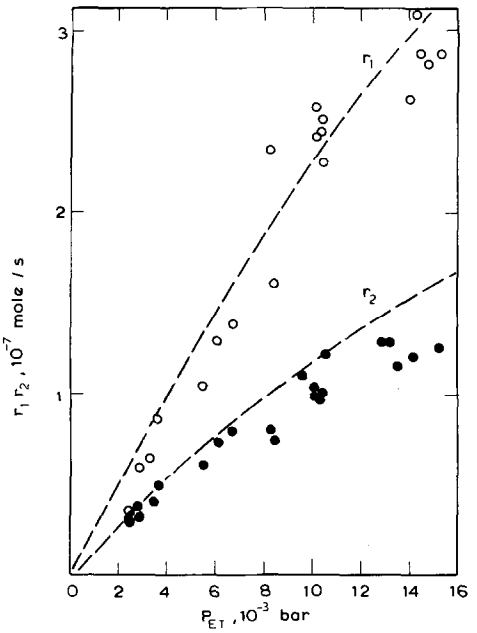

FIG. 6. Rates of ethylene epoxidation (r_1) and combustion (r_2) vs P_{ET} at 300°C. Broken lines from Eqs. (10)–(14).

reactor the electrochemically measured surface oxygen activity a_O^2 (Eq. (6)) was always found to equal P_{O_2} within 1–2%. However in the presence of ethylene, i.e.,

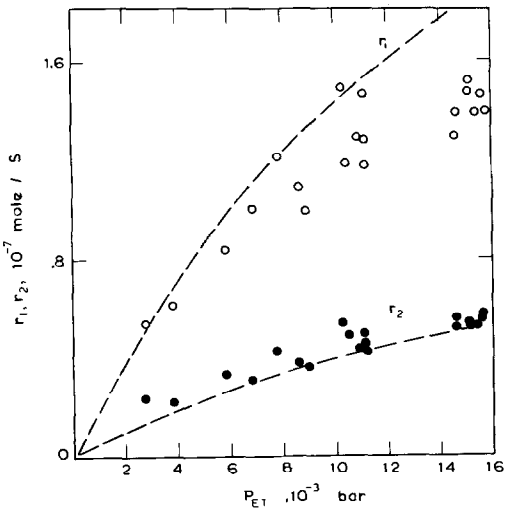

FIG. 7. Rates of ethylene epoxidation (r_1) and combustion (r_2) vs P_{ET} at 250°C. Lines correspond to Eqs. (10)–(14).

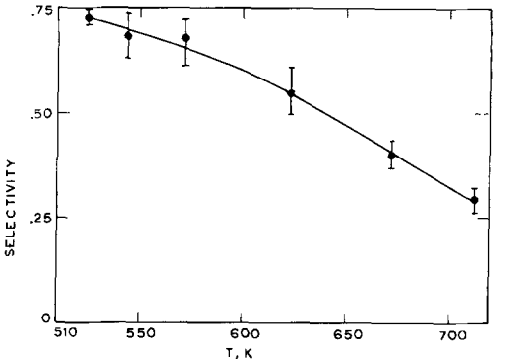

FIG. 8. Temperature dependence of the selectivity (moles ethylene oxide produced/moles ethylene reacted).

during reaction, open-circuit emf values between -20 and -100 mV are obtained and thus, in general, $a_O^2 < P_{O_2}$. This implies that no thermodynamic equilibrium is established between gaseous oxygen and oxygen adsorbed on silver under reaction conditions. It was observed that

(a) a_O^2 approaches P_{O_2} with increasing temperature at constant P_{O_2} and P_{ET};

(b) a_O^2 increases with increasing P_{O_2} at constant P_{ET};

(c) a_O^2 decreases with increasing P_{ET} at constant P_{O_2};

(d) varying the partial pressure of ethylene oxide P_{ETOX} causes a very small change (2–3 mV) on the emf at constant P_{ET} and P_{O_2} to the extent that P_{ETOX} is below 0.02 bar. Carbon dioxide has no effect whatsoever (<1 mV) on a_O.

Observation (b) is in agreement with Imre's previous work but observation (c) is not. Imre suggested that the oxygen activity increases with increasing P_{ET}. It should be noted however that his definition of oxygen activity is different from Eq. (5) and that his method of measurement is quite indirect (*23*).

Several functional forms were examined in order to describe the dependence of a_O on gas-phase composition. It was found that all the a_O measurements could be correlated in a quite satisfactory way by the expression

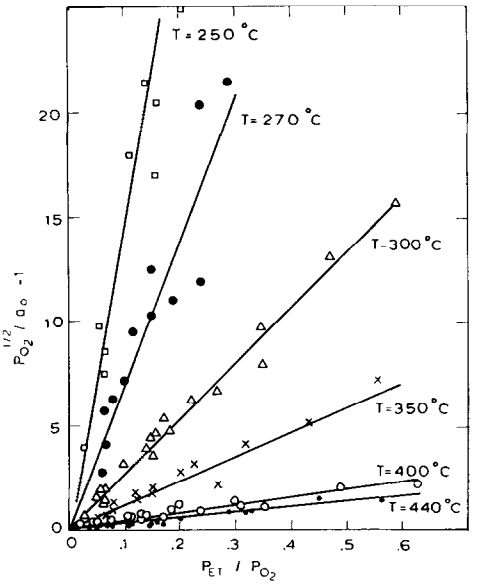

FIG. 9. Surface oxygen activity dependence on gas-phase composition.

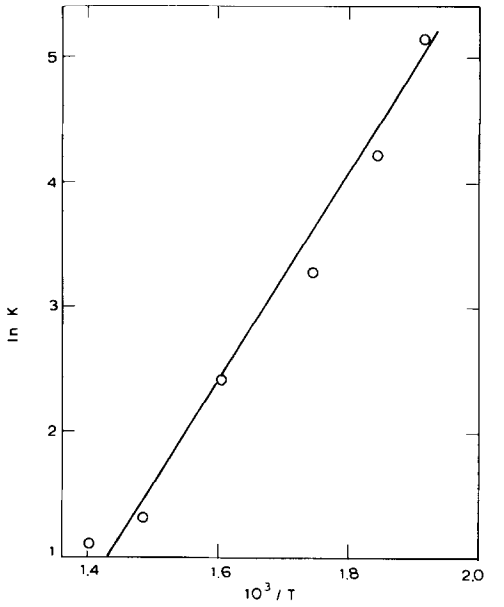

FIG. 10. Temperature dependence of the oxygen activity parameter K (Eqs. (15), (15a)).

$$P_{O_2}^{1/2}/a_O = 1 + KP_{ET}/P_{O_2} \qquad (15)$$

with

$$K = 3.4 \cdot 10^{-5} \exp(7800/T). \qquad (15a)$$

This is shown in Figs. 9 and 10.

The defining Equation (5) of the activity a_O of surface oxygen atoms does not imply that oxygen adsorbs in the form of atoms only. It is well established (*1, 13, 30, 31*) that several forms of adsorbed oxygen can exist on silver. To the extent that all these forms are in thermodynamic equilibrium, i.e., they all have the same steady-state chemical potential, then the emf E and thus a_O reflect this common chemical potential. If, however, due to fast kinetic processes, such an equilibrium is not established then the emf E reflects the activity of oxygen atoms as they are the fastest ones to equilibrate with the O^{2-} of the solid electrolyte (*20*). This is further discussed below.

The Effect of CO_2

The effect of CO_2 on the rate of ethylene epoxidation and combustion as well as on the surface oxygen activity a_O was studied at temperatures between 250 and 400°C and partial pressures of CO_2 between 0.5 bar and $3 \cdot 10^{-4}$ bar. The partial pressure of ethylene was varied between $0.5 \cdot 10^{-2}$ and $1.6 \cdot 10^{-2}$ bar and that of oxygen between $3. \cdot 10^{-2}$ and $12 \cdot 10^{-2}$ bar.

Figure 11 shows the inhibiting effect of CO_2 and r_1 at $P_{ET} = 1.3 \cdot 10^{-2}$ bar and P_{O_2} between 0.05 and 0.1 bar for the various temperatures examined; r_1° is the rate of ethylene epoxidation in the absence of excess CO_2, except that produced by reaction, which corresponds to P_{CO_2} usually less than 10^{-3} bar. Figure 11 shows that CO_2 has a pronounced inhibiting effect on r_1 at temperatures below 330°C.

No single correlation of r_1/r_1° with P_{CO_2} was found to hold when P_{O_2} varies. Although over the range of parameters investigated r_1 is zero order in oxygen for low P_{CO_2}, it was found that the rate increases considerably with increasing P_{O_2} at constant ethylene and constant high values of P_{CO_2} (>0.05 bar). Careful examination of the data showed that r_1/r_1° could be uniquely related to the ratio P_{CO_2}/P_{O_2} at

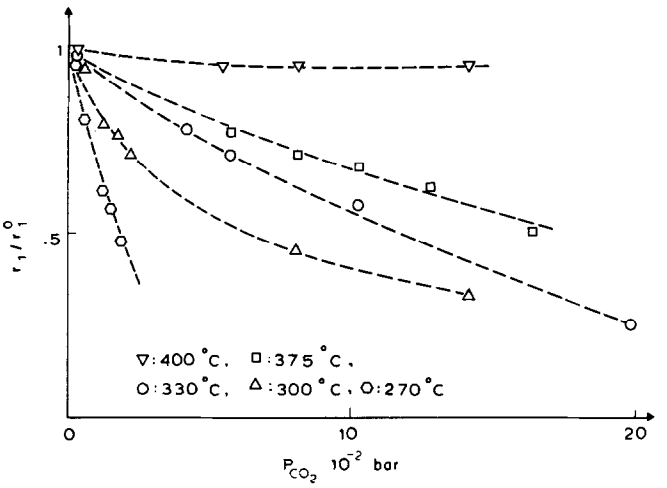

FIG. 11. Effect of CO_2 on the rate of ethylene epoxidation r_1.

constant T:

$$r_1^\circ/r_1 = 1 + K'P_{CO_2}/P_{O_2}. \qquad (16)$$

This is shown in Fig. 12, where $(r_1^\circ/r_1)-1$ is plotted vs P_{CO_2}/P_{O_2}. The temperature dependence of the proportionality constant K' is shown in Fig. 13. The parameter K' increases with decreasing temperature since the CO_2 retarding effect on r_1 is significant below 330°C and almost vanishes above 400°C.

Similarly with the ethylene oxidation experiments at low P_{CO_2} values, it was found that the surface oxygen activity a_O is uniquely defined by P_{ET}, P_{O_2}, and T and is totally independent of P_{CO_2}. This is shown in Fig. 14 for various temperatures and gas-phase compositions. The oxygen activity a_O remains constant within 2% as P_{CO_2} varies more than three orders of magnitude. This is remarkable in view of the fact that at the same time r_1 is decreasing considerably (Fig. 11).

Within the accuracy of the experimental measurements the rate of ethylene combustion r_2 remains virtually constant with increasing P_{CO_2}. This is shown in Fig. 15 where r_1°/r_1 and r_2°/r_2 are compared at constant T, P_{ET}, and P_{O_2}. As shown in the figure the measurement of r_2 is subject to considerable experimental error for high P_{CO_2} values because in this region the ir CO_2 analyzer could not be used and the chromatographic separation of the ethylene peak and the large CO_2 peak was not complete. However, one can definitely conclude that if CO_2 has an effect on r_2 the effect is much smaller than the corresponding one for r_1. This is in agreement with previous work by Hayes

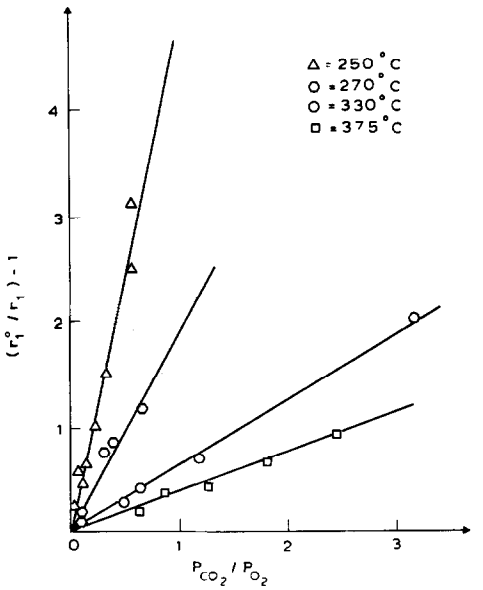

FIG. 12. Effect of the P_{CO_2}/P_{O_2} ratio on the rate of ethylene epoxidation r_1.

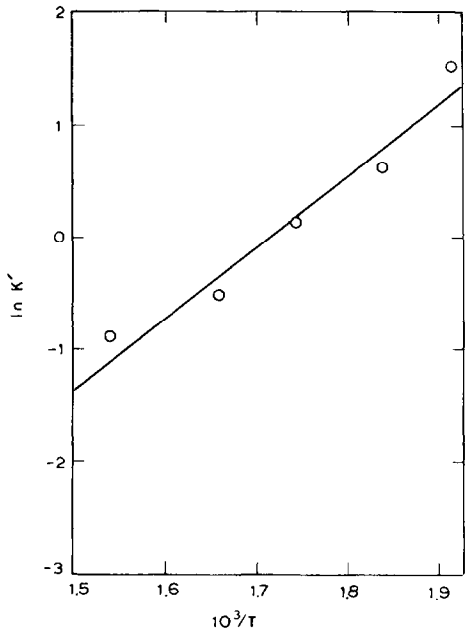

FIG. 13. Temperature dependence of K'.

(*17*) and Nault (*34*) although other workers have reported that CO_2 inhibits r_2 also (*18, 35*).

DISCUSSION

Since the early work of Twigg (*10, 11*) a number of reaction mechanisms have been proposed for ethylene oxidation on Ag. We can discuss now some of these mechanisms on the basis of the reaction network kinetics, previous experimental investigations, and the new information provided by the solid-electrolyte-aided surface oxygen activity measurement.

Twigg basically proposed an Eley–Rideal-type mechanism between gaseous ethylene and atomically adsorbed oxygen (*10, 11*). According to this early mechanism, reaction of ethylene with one adsorbed oxygen atom gives C_2H_4O, while reaction of C_2H_4 with two oxygen atoms gives CO_2. Since this early work a number of studies have shown that several forms of adsorbed oxygen exist on silver during ethylene oxidation (*1, 13, 30, 31*). According to the classical picture of Kilty and Sachtler one of these forms of oxygen, i.e., molecularly adsorbed O_2, gives rise to ethylene oxide while atomically adsorbed oxygen yields CO_2 (*1, 2*). This mechanism can also explain the observed increase in selectivity when trace amounts of chlorinated hydrocarbons are added to the feedstream (*2*). Furthermore, Twigg's early notions of an Eley–Rideal-type mechanism do not seem to be well accepted by the majority of previous workers (*13, 16*) as recent ir spectroscopic studies have shown several species adsorbed on Ag during ethylene oxidation including at least two forms of oxygen,

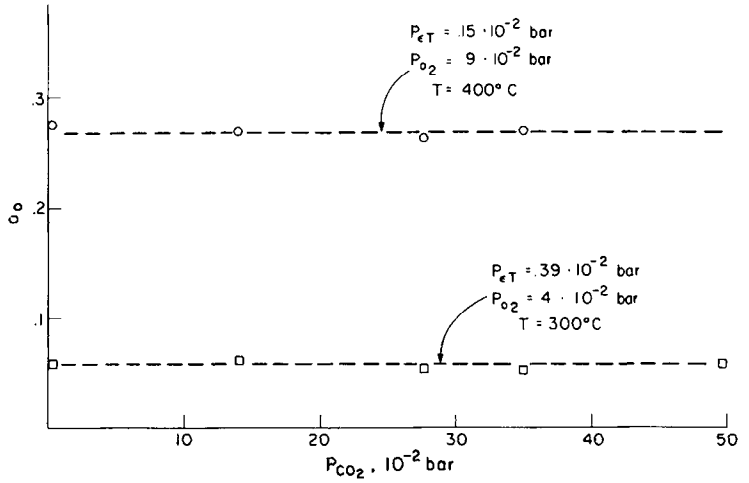

FIG. 14. Surface oxygen activity a_O vs P_{CO_2}.

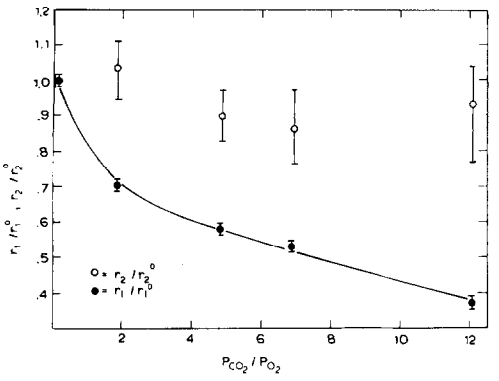

FIG. 15. Effect of CO_2 on r_1 and r_2 at constant T, P_{ET}, and P_{O_2}.

ethylene, CO_2, and ethylene oxide as well as oligomers of ethylene oxide (*6, 7*).

The present results including the surface oxygen activity data can be accounted for within the general framework of the Kilty–Sachtler mechanism. In agreement with previous work we found it necessary to postulate the existence of two types of adsorbed oxygen in order to explain the experimental observations presented here. A strong indication of the existence of two types of adsorbed oxygen is the retarding effect of CO_2 (Figs. 14 and 15). Carbon dioxide retards r_1 only and leaves r_2 and the emf almost totally unaffected. It thus follows that CO_2 competes for the same adsorption sites with the oxygen species responsible for ethylene oxide formation but not with the oxygen species the activity of which is being electrochemically measured and which produces CO_2. Since the emf measurements are expected to reflect the activity of atomic oxygen (*20*) it would follow that atomic oxygen is responsible for CO_2 formation while a second type of oxygen, presumably molecularly adsorbed, yields ethylene oxide, in excellent agreement with what previous workers have proposed (*1, 2, 23*).

A satisfactory mechanism for ethylene oxidation should account not only for the kinetics (Eqs. (10) and (11)) but also for the surface oxygen activity behavior (Eq. (15)). Such a mechanism explaining all the experimental observations in a semiquantitative manner is presented below.

According to the previous discussion we assume two types of surface sites S_2 and S_3 for atomic and molecular oxygen adsorption, respectively. We also assume the existence of a third type of site S_1 for ethylene and ethylene oxide chemisorption. In order to account for the above-mentioned CO_2 effect carbon dioxide must then compete with molecular oxygen for S_3 sites. We assume Langmuir-type adsorption for ethylene on S_1 sites and thermodynamic equilibrium between surface and gaseous ethylene during reaction. It thus follows that the coverage θ_{ET} of ethylene on S_1 sites is given by

$$\theta_{ET} = K_{ET}P_{ET}/(1 + K_{ET}P_{ET}), \quad (17)$$

where K_{ET} is the adsorption coefficient of ethylene, provided P_{ETOX} is small enough (<0.02 bar) so that (*12*) $\theta_{ETOX} \approx 0$.

Similarly, assuming Langmuir-type adsorption for molecular oxygen on S_3 sites and thermodynamic equilibrium between molecularly adsorbed and gaseous O_2 one obtains

$$\theta_{O_2} = K_{O_2}P_{O_2}/(1 + K_{O_2}P_{O_2}), \quad (18)$$

where θ_{O_2} is the O_2 coverage of S_3 sites and K_{O_2} is the molecular adsorption coefficient of oxygen. If P_{CO_2} is high (>0.05 bar) and the temperature low, then (18) would have to be modified in the form

$$\theta_{O_2} = K_{O_2}P_{O_2}/(1 + K_{O_2}P_{O_2} + K_{CO_2}P_{CO_2}). \quad (19)$$

We will also assume Langmuir-type adsorption of atomic oxygen on S_2 sites but will not necessarily assume thermodynamic equilibration between gaseous and atomically adsorbed oxygen. This is possible if the atomic oxygen adsorption–desorption kinetics are relatively slow with respect to the surface reaction. Because of the definition of surface oxygen activity a_O (Eq. (5)) and the Langmuir adsorption assumption it follows that

$$\theta_O = K_O a_O/(1 + K_O a_O). \quad (20)$$

Note that this expression relates two intrinsic surface properties and is valid whether or not equilibrium with the gas phase exists. If such an equilibrium exists, then $P_{O_2} = a_O^2$ by definition and (20) reduces to the common form of the Langmuir isotherm for dissociative adsorption.

On the basis of these assumptions it follows that the rate of ethylene oxide formation r_1 is given by

$$r_1 = K_1 \theta_{ET} \theta_{O_2} = K_1 \frac{K_{ET} P_{ET}}{1 + K_{ET} P_{ET}} \cdot \frac{K_{O_2} P_{O_2}}{1 + K_{O_2} P_{O_2}} \quad (21)$$

which reduces to the experimental rate expression (10) if $K_{O_2} P_{O_2} \gg 1$. This is quite reasonable since all the experiments were performed with $P_{O_2} > 1.5 \cdot 10^{-2}$ bar. It is reasonable to expect that for very low values of P_{O_2} the rate r_1 will become first order in oxygen.

Similarly, the rate of ethylene deep oxidation r_2 is given by

$$r_2 = K_2 \cdot \theta_{ET} \cdot \theta_O = K_2 \frac{K_{ET} P_{ET}}{1 + K_{ET} P_{ET}} \cdot \frac{K_O a_O}{1 + K_O a_O} \quad (22)$$

which reduces to the experimental expression (11) if $K_O a_O \gg 1$. It should be noted that $\theta_O \approx 1$ is not inconsistent with the experimental observation $a_O^2 < P_{O_2}$ to the extent that $K_O a_O \gg 1$. SEP measurements are quite sensitive to changes in the activity of oxygen at near surface saturation because of the exponential dependence of a_O on the measured emf (Eq. (6)). Thus a_O can change by orders of magnitude while θ_O remains close to unity as long as $K_O a_O \gg 1$ as is the case here. From (*21*) and (*10*) it follows that the experimentally determined parameter K_{ET} (Fig. 16) is the adsorption coefficient of ethylene on silver. According to Eq. (14) it follows that the enthalpy and entropy of adsorption of ethylene on silver are $\Delta H_{ET} = -11.5$ kcal/mole and $\Delta S_{ET} = -14$ cal/mole · K. Both values are quite reasonable and in good agreement with those reported by Dettwiller (*16*).

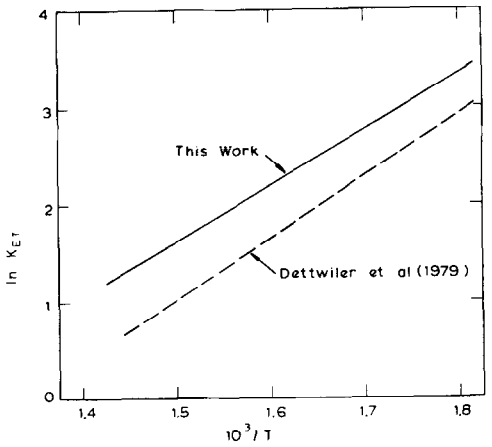

FIG. 16. Temperature dependence of ethylene adsorption coefficient K_{ET}.

The difference in activation energies of K_2 and K_1 (22. − 14.5 = 7.5 kcal/mole) explains well the monotonic drop in selectivity with increasing temperature (Fig. 8).

The surface oxygen activity dependence on temperature and gas-phase composition can be explained now by considering a steady-state mass balance for adsorbed atomic oxygen:

$$O = K_{ad} \cdot P_{O_2}^{1/2} \cdot (1 - \theta_O)(1 - \theta_{ET}) - K_d \cdot \theta_O (1 - \theta_{ET}) - \gamma \cdot K_2 \theta_{ET} \theta_O + K_1 \theta_{ET} \theta_{O_2}. \quad (23)$$

The first term corresponds to the atomic oxygen adsorption step using the same assumptions made in the ethylene oxide study (*12*), i.e., that atomic oxygen adsorption on a S_2 site requires an empty adjacent S_1 site. The second term corresponds to oxygen desorption under the same assumptions. Note that in the absence of ethylene ($\theta_{ET} = 0$) the last two terms vanish and Eq. (13) reduces to the common form of the Langmuir isotherm with $K_O = K_{ad}/K_d$. The third term refers to atomic oxygen reacting with ethylene to form CO_2. The coefficient γ would equal 6 if all oxygen contained in CO_2 is originally atomically adsorbed. However since some of that oxygen may originate from the gas phase once an acti-

vated complex between adsorbed ethylene and adsorbed atomic oxygen is formed we will leave γ unspecified and treat it as an adjustable parameter. The last term accounts for atomic oxygen formed from molecular oxygen. We assume that whenever ethylene reacts with molecularly adsorbed oxygen to form ethylene oxide, the oxygen atom thus formed migrates to an atomic oxygen adsorption site S_2.

Taking into account Eqs. (17) and (20) and dividing (23) by $K_{ad}(1 - \theta_O)$ $(1 - \theta_{ET})a_O$ one obtains

$$\left(\frac{P_O^{1/2}}{a_O} - 1\right)\theta_O = \frac{K_1}{K_d} \cdot K_{ET} \cdot P_{ET} \cdot \left[\frac{\gamma K_2}{K_1}\theta_O - \theta_{O_2}\right] \quad (24)$$

and taking into account that $\theta_O \approx 1$ according to the kinetics (Eq. (11)):

$$P_O^{1/2}/a_O = 1 + \frac{K_1 K_{ET}}{K_d} P_{ET}\left[\frac{\gamma K_2}{K_1} - \theta_{O_2}\right]. \quad (25)$$

The ratio K_2/K_1 is of order 1. It varies from roughly 2 at 440°C to ~0.5 at 250°C. Agreement with experiment becomes quantitative if $\gamma K_2/K_1 \approx 1$. This assumption is not unreasonable but cannot be justified independently. With this assumption and according to Eq. (18) it follows that

$$1 - \theta_{O_2} = 1/K_{O_2}P_{O_2} \quad (26)$$

and Eq. (25) reduces to the experimental expression

$$P_{O_2}^{1/2}/a_O = 1 + KP_{ET}/P_{O_2} \quad (15)$$

which describes the surface oxygen activity behavior, with

$$K = K_{ET}K_1/K_{O_2}K_d. \quad (27)$$

Figure 10 shows the temperature dependence of K which corresponds to Eq. (15a). The temperature dependence of K_{ET} and K_1 is described by Eqs. (14) and (12), respectively. One could thus estimate ΔH_{O_2}, the heat of oxygen molecular adsorption, from K_{O_2} if the activation energy of K_d were known. By using an average literature value of ~28 kcal/mole (*1, 32*) for the rate coefficient of atomic oxygen desorption one estimates $\Delta H_{O_2} = -9.5$ kcal/mole, in agreement with the calorimetric data of Ostrovskii *et al.* at high oxygen coverages (*31*).

In the above analysis which explains the experimental observations (10), (11), and (15) the effect of CO_2 on r_1 has been neglected.

Since CO_2 competes with molecular oxygen only, the rate of ethylene combustion r_2 given by (22) should remain unchanged in agreement with experiment. However, the coverage of O_2 on molecular oxygen and carbon dioxide adsorption sites becomes

$$\theta_{O_2} = \frac{K_{O_2}P_{O_2}}{1 + K_{O_2}P_{O_2} + K_{CO_2}P_{O_2}} \approx \frac{K_{O_2}P_{O_2}}{K_{O_2}P_{O_2} + K_{CO_2}P_{CO_2}}, \quad (28)$$

where K_{CO_2} is the adsorption coefficient of CO_2. The last equation is valid as long as $K_{O_2}P_{O_2} \gg 1$. It thus follows from (21) that

$$r_1^\circ/r_1 = 1 + \frac{K_{CO_2}}{K_{O_2}}\frac{P_{CO_2}}{P_{O_2}} \quad (29)$$

provided r_1 and r_1° are measured at the same P_{ET}. This is the experimentally obtained relation (16) if $K' = K_{CO_2}/K_{O_2}$. Thus the parameter $K' = 1.2 \cdot 10^{-5} \cdot \exp(6600/T)$ can be interpreted as a ratio of two adsorption coefficients.

This would imply $\Delta H_{CO_2} - \Delta H_{O_2} \approx -13.1$ kcal/mole, where ΔH_{CO_2} and ΔH_{O_2} are the heats of adsorption of CO_2 and molecular O_2, respectively. If $\Delta H_{O_2} \approx -10$ kcal/mole (*31*) one obtains $\Delta H_{CO_2} \approx -23$ kcal/mole. The difference $\Delta H_{CO_2} - \frac{1}{2}\Delta H_{O_2}$ of the two heats of adsorption is -18 kcal/mole, quite close to the $\Delta H°$ of the reaction

$$Ag_2O + CO_2 \rightarrow Ag_2CO_3 \quad (30)$$

which is -18.5 kcal/mole at 298 K. Although this may be coincidental it does suggest the possibility of CO_2 forming sur-

face carbonate by adsorbing on oxygen atoms trapped in molecular oxygen adsorption sites after reaction of molecular oxygen with ethylene to form ethylene oxide. This is supported by the results of Force and Bell's study (*6, 7*) who observed surface carbonate formation upon chemisorption of CO_2 on Ag in the presence of O_2, as well as by those of Czanderna who reports that CO_2 adsorbs on silver only when the surface is partially oxidized (*32*).

In summary, the oxygen activity measurements provide some new information about ethylene oxidation on silver. The use of solid-electrolyte potentiometry in conjunction with other surface-sensitive techniques, such as ir spectroscopy, could improve considerably the understanding of this important catalytic system.

ACKNOWLEDGMENTS

The research was supported under NSF Grant ENG 77-27500. Acknowledgment is also made to the Donors of the PRF, administered by the ACS for partial support of this research under Grant 9893-G3. We also thank Mobil, DuPont, and Union Carbide for partial support of this research.

REFERENCES

1. Kilty, P. A., and Sachtler, W. M. H., *Catal. Rev. Sci. Eng.* **10**(1), 1 (1974).
2. Kilty, P. A., Rol, N. C., and Sachtler, W. M. H., *in* "Proceedings, 5th International Congress on Catalysis, Miami" (J. W. Hightower, Ed.), Paper 64, p. 929. Amer. Elsevier, New York, 1972.
3. Carberry, J. J., Kuczynski, G. C., and Martinez, E., *J. Catal.* **26**, 247 (1972).
4. Cant, N. W., and Hall, W. K., *J. Catal.* **52**, 81 (1978).
5. Larrabee, A. L., and Kuczkowski, R. L., *J. Catal.* **52**, 72 (1978).
6. Force, E. L., and Bell, A. T., *J. Catal.* **38**, 440 (1975).
7. Force, E. L., and Bell, A. T., *J. Catal.* **40**, 356 (1975).
8. Wu, J. C., and Harriot, P., *J. Catal.* **39**, 395 (1975).
9. Korchak, V. N., and Tretyakov, J. J., *Kinet. Katal.* **18**(1), 141 (1977).
10. Twigg, G. H., *Proc. Roy. Soc. Ser. A* **188**, 92 (1946).
11. Twigg, G. H., *Trans. Faraday Soc.* **42**, 284 (1946).
12. Stoukides, M., and Vayenas, C. G., *J. Catal.* **64**, 18 (1980).
13. Voge, H. H., and Adams, C. R., *in* "Advances in Catalysis and Related Subjects," Vol. 17, p. 154. Academic Press, New York/London, 1967.
14. Kummer, J. T., *J. Phys. Chem.* **60**, 66 (1956).
15. Harriot, P., *J. Catal.* **21**, 56 (1971).
16. Dettwiller, H. D., Baiker, A., and Richarz, W., *Helv. Chim. Acta* **62**, 1689 (1979).
17. Hayes, K. E., *Can. J. Chem.* **38**, 2256 (1960).
18. Kurilenko, A. I., *et al.*, *Zh. Fiz. Khim.* **32**, 1048 (1958).
19. Temkin, M. I., *Kinet. Katal.* **18**(3), 544 (1977).
20. Wagner, C., *in* "Advances in Catalysis and Related Subjects," Vol. 21, p. 323. Academic Press, New York/London, 1970.
21. Vayenas, C. G., and Saltsburg, H. M., *J. Catal.* **57**, 296 (1979).
22. Vayenas, C. G., Lee, B., and Michaels, J., *J. Catal.* **66**, 36 (1980).
23. Imre, L., *Ber. Bunsenges. Phys. Chem.* **74**, 220 (1970).
24. Pancharatnam, S., Huggins, R. A., and Mason, D. M., *J. Electrochem. Soc.* **122**, 869 (1975).
25. Vayenas, C. G., and Farr, R. D., *Science* **208**, 593 (1980).
26. Farr, R. D., and Vayenas, C. G., *J. Electrochem. Soc.* **127**(7), 1478 (1980).
27. Stoukides, M., and Vayenas, C. G., *J. Catal.*, in press (1981).
28. Dietz, H., Haecker, W., and Jahnke, H., *in* "Advances in Electrochemistry and Electrochemical Engineering" (H. Gerischer and C. W. Tobias, Eds.), Vol. 10, p. 1. Wiley-Interscience, New York, 1977.
29. Kleitz, M., Fabry, P., and Schoule, E., *in* "Electrode Processes in Solid State Ionices" (M. Kleitz and J. DuPuy, Eds.). Reidel, Dordrecht, 1976.
30. Spath, H. T., *in* "Proceedings, 5th International Congress on Catalysis, Miami" (J. W. Hightower, Ed.), Paper 64, p. 929. Amer. Elsevier, New York, 1972.
31. Ostrovskii, V. E., and Temkin, M. I., *Kinet. Katal.* **7**(3), 529 (1966).
32. Czanderna, A. W., *J. Colloid. Interface Sci.* **24**, 500 (1967).
33. McKim, F. L., and Cambron, A., *Can. J. Res. Sect. B* **27**, 814 (1949).
34. Nault, G. N., *et al.*, *Ind. Eng. Chem. Process Des. Develop.* **1**, 285 (1962).
35. Metcalf, P. L., and Harriot, P., *Ind. Eng. Chem. Process Des. Develop.* **11**, 4 (1972).